GEM TN-93-353

Joule Heating of GEM Detector Bobbin Cooling Tubes

A. Radovinsky
Plasma Fusion Center-Massachusetts Institute of Technology

March 8, 1993

Abstract:

Joule heating of GEM detector magnet bobbins was analyzed in [2] without considering effects due to the presence of the thermosiphon cooling tubes. The results presented in this memo show that the impact of the tubing on the results of the above mentioned memo is small. They also show the currents and power deposition in the tubing jumpers between the quadrant segments to be negligible.

MIT-GEM-EM-16

Joule Heating of GEM Detector Bobbin Cooling Tubes

08 March 1993

A. Radovinsky

This document and all reports and memoranda in this series are intended as a record of work in progress. They are for use in informal discussions of design and fabrication alternatives. This material is subject to change and should not, therefore, be published or referred to in the open literature. Conclusions are preliminary and distribution should be strictly limited.

Plasma Fusion Center
Massachusetts Institute of Technology
Cambridge, MA 02139

MIT GEM Detector Memoranda
Approval Sheet

B.A. Smith
Project Engineer

3/9/93
Date

R.D. Pillsbury, Jr.
Technical Monitor

3/9/93
Date

A.M. Dawson
Technical Editor

Date

MIT-GEM-EM-016

Memorandum

TO: B.Smith

CC: R.D.Pillsbury
File

FROM: Alexi Radovinsky

DATE: Feb. 19, 1993

SUBJ: Joule Heating of GEM Detector Bobbin Cooling Tubes

ABSTRACT

Joule heating of GEM detector magnet bobbins was analyzed in [2] without considering effects due to the presence of the thermosiphon cooling tubes. The results presented in this memo show that the impact of the tubing on the results of the above mentioned memo is small. They also show the currents and power deposition in the tubing jumpers between the quadrant segments to be negligible.

ANALYSIS

The program EDDYCUFF[1] was used in these analyses. EDDYCUFF assumes that the conducting medium is a shell which is thin relative to the skin depth, which implies a uniform distribution of current density through the thickness of the material. This also implies that there is no current flow perpendicular to the plane of the shell. The dimensions of the model are shown in Fig. 1. An axial cross section of a set of 12 cylindrical coil modules and thin conducting bobbins is shown, with axial symmetry about the Z-axis and a plane of symmetry at Z=0.

The bobbin quadrant segments were modeled as four cylindrical shells (AB, BC, CD, and, DA) shown in Fig. 2, with a centroid radius of 9.582 m, thickness of 0.076 m, and length in the Z-direction of 1.1875 m. The segments had 0.0508 m gaps between each other (at points A, B, C, and D). To take into account the flange contribution to the shell conductivity, an additional thickness, equivalent to the cross section of a flange (0.026 m^2), was added to the bobbin elements at each end of the bobbin section.

According to the assumption that there are three tubes per quadrant, the tubing jumpers shown at points B, C, and D in Fig. 3 were modeled by three lines of elements with a cross section of $1.94*10^{-4}$ m^2 each connecting the segments at points B, C, and D in Fig. 2. The impact of the tubes in the areas where they overlay the segments was neglected since their effective cross section is much less than that of the bobbin walls to which the tubes are electrically connected. No jumpers were introduced into the model between the segments at point A, leaving a single circumferential electrical break.

The resistivity of the material was assumed to be $1.4*10^{-8}$ ohm*m, which corresponds to Al 6061 at 4-4.5 K.

The coils were modeled as uniform current density solenoids with a centroid radius of 9.5 m, thickness of 0.02 m, and length in Z-direction of 0.9709 m. The current (I) in all solenoids is the same, corresponding to discharge, with an exponential current decay characterized by a time constant of 100 s. That is

$$I=950*\exp(-t/100) \quad kA$$

Only the effects in the 12-th bobbin were analyzed. As was shown in [2] this comprises about 48% of the heating of all the 12 bobbins of half the magnet.

RESULTS

The comparison of the power deposition in the model (Fig. 2) with tubes to the power deposition in the model [2] without tubes shows a very small difference (see Fig. 4). This difference may arise in part from the different mesh configurations used in the two cases rather than from the actual impact of the added tubing. Thus it can be considered that as regards the heating of the bobbin quadrants the results published in [2] are quite appropriate and do not need verification with respect to the presence of the tubing provided the plumbing scheme corresponds to the model (Fig. 3) used in this study.

The distribution of eddy currents in the entire model at t=9 seconds is shown in Fig. 5. The general patterns of eddy currents in the bobbin walls are visually the same as in the corresponding case without tubes (see Fig. 5.d. of reference [2]) with small distortions in the vicinities of the edges interconnected by the tubes. Figure 6 shows the eddy currents in the elements modeling the tubing jumpers at points A, B, and C. In each triplet of the tubing jumpers the currents in the outer ones are opposite. The currents in all these jumpers are approximately equal and they substantially exceed those in the central jumpers.

Figures 7 and 8 show the current density and the power deposition in a typical outer tubing jumper versus time. The heat load is clearly negligible.

---

[1] *EDDYCUFF User's Manual ... (To be published)*

[2] *Alexi Radovinsky, Joule Heating of GEM Detector Bobbins, MIT-GEM-EM-014, (internal report), December 1992.*

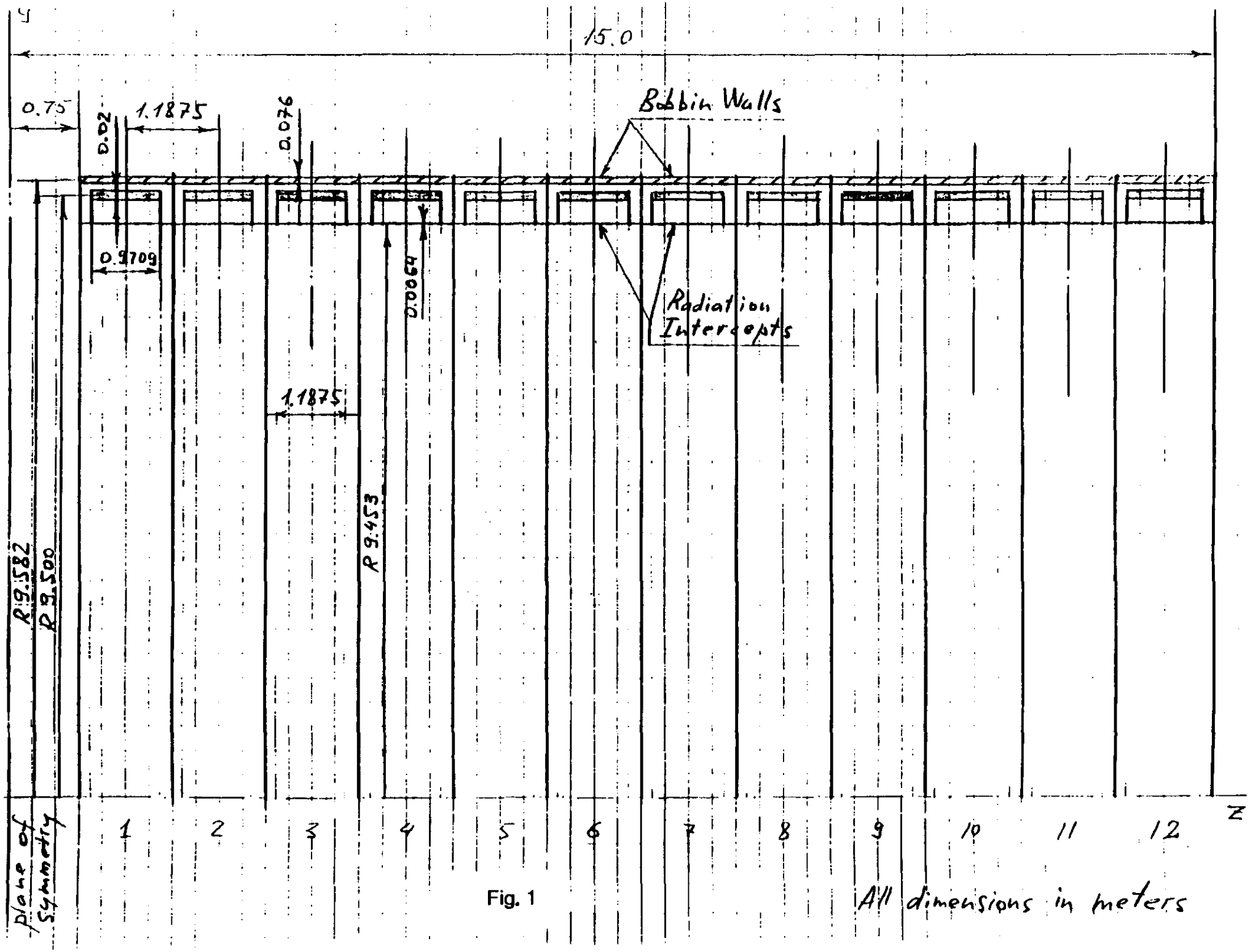
15.0
0.75
1.1875
0.02
0.076
Bobbin Walls
0.9709
0.0064
Radiation Intercepts
1.1875
R 9.582
R 9.500
R 9.453
Plane of Symmetry
1
2
3
4
5
6
7
8
9
10
11
12
z
All dimensions in meters

Fig. 1

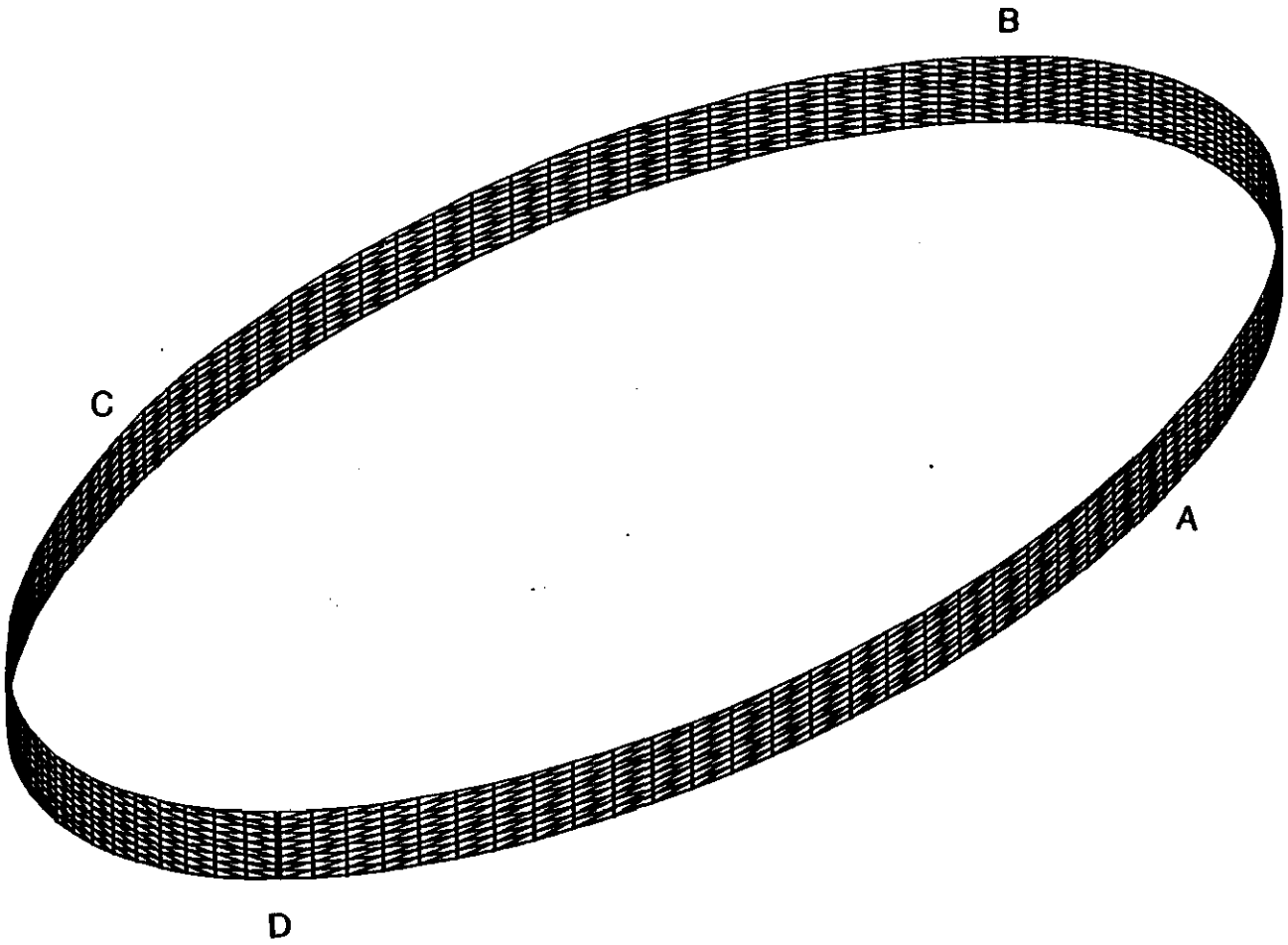

Fig. 2 GEM Detector Magnet 12-th Bobbin Finite Element Model

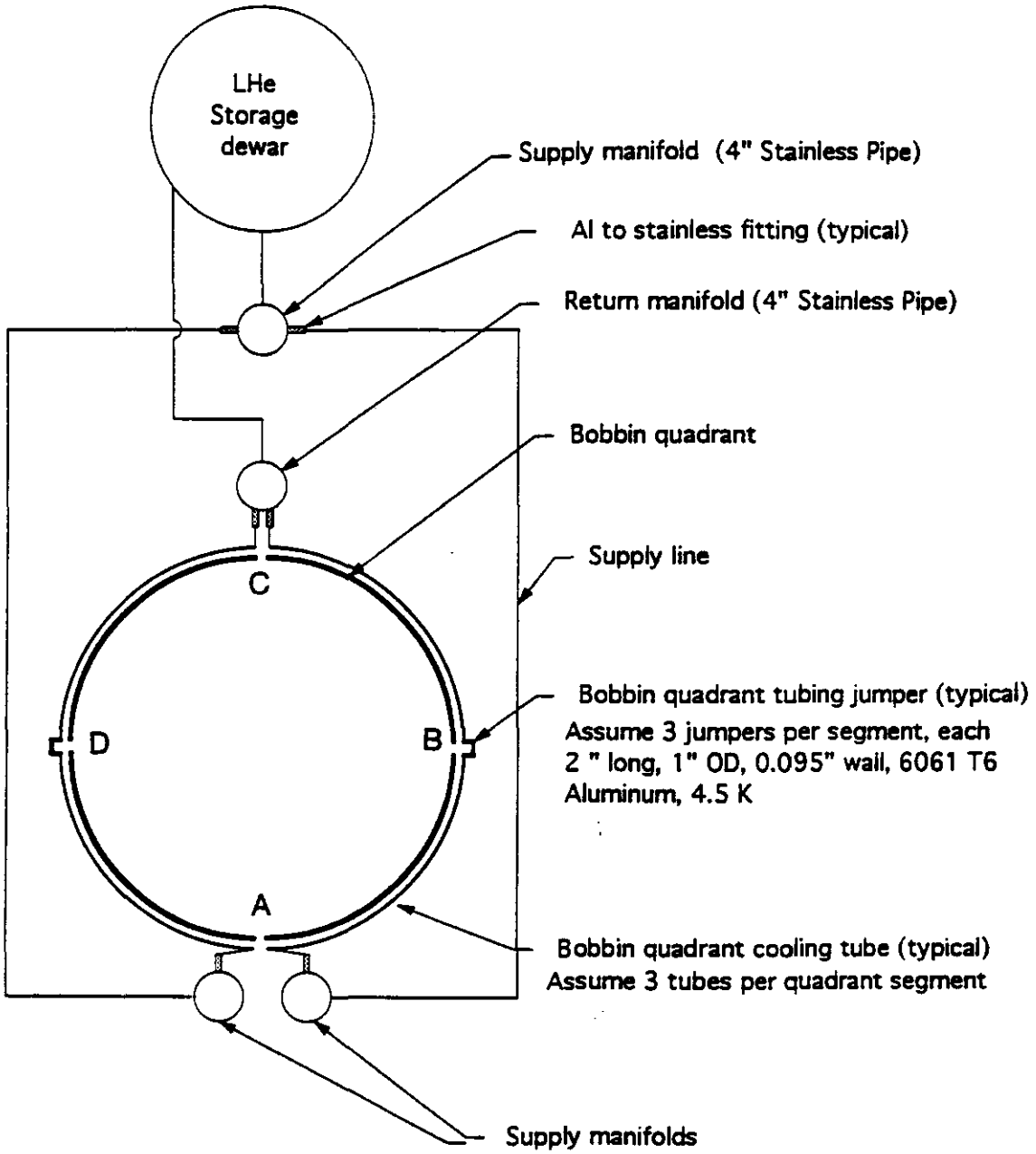

Fig. 3 Thermosiphon Plumbing for Eddy Current Analysis

BAS
2/9/93

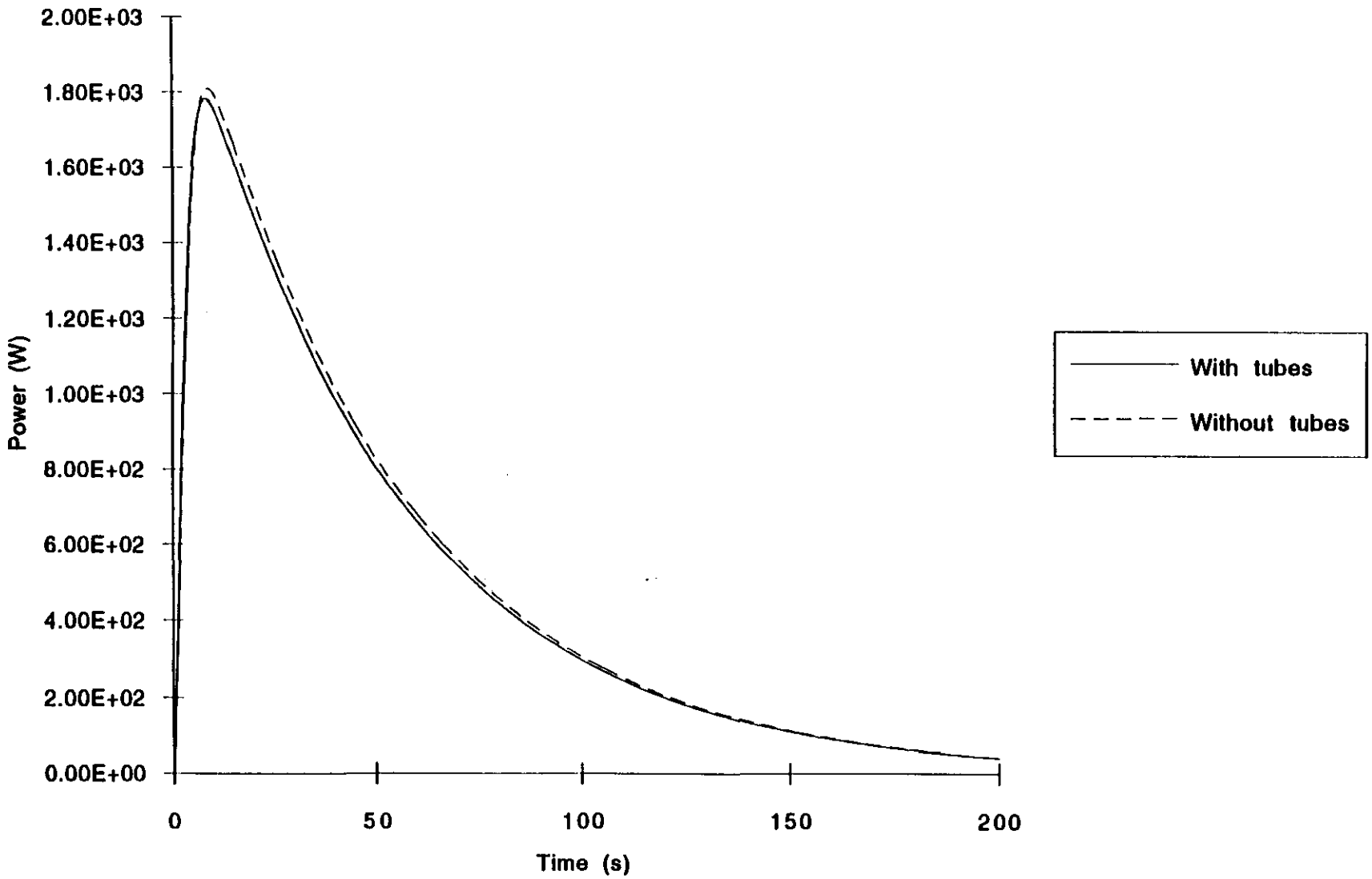

Fig. 4 Power Deposition in the 12-th Bobbin during Discharge

Fig. 5 Distribution of Current Density in the 12-th Bobbin at t=9 s.

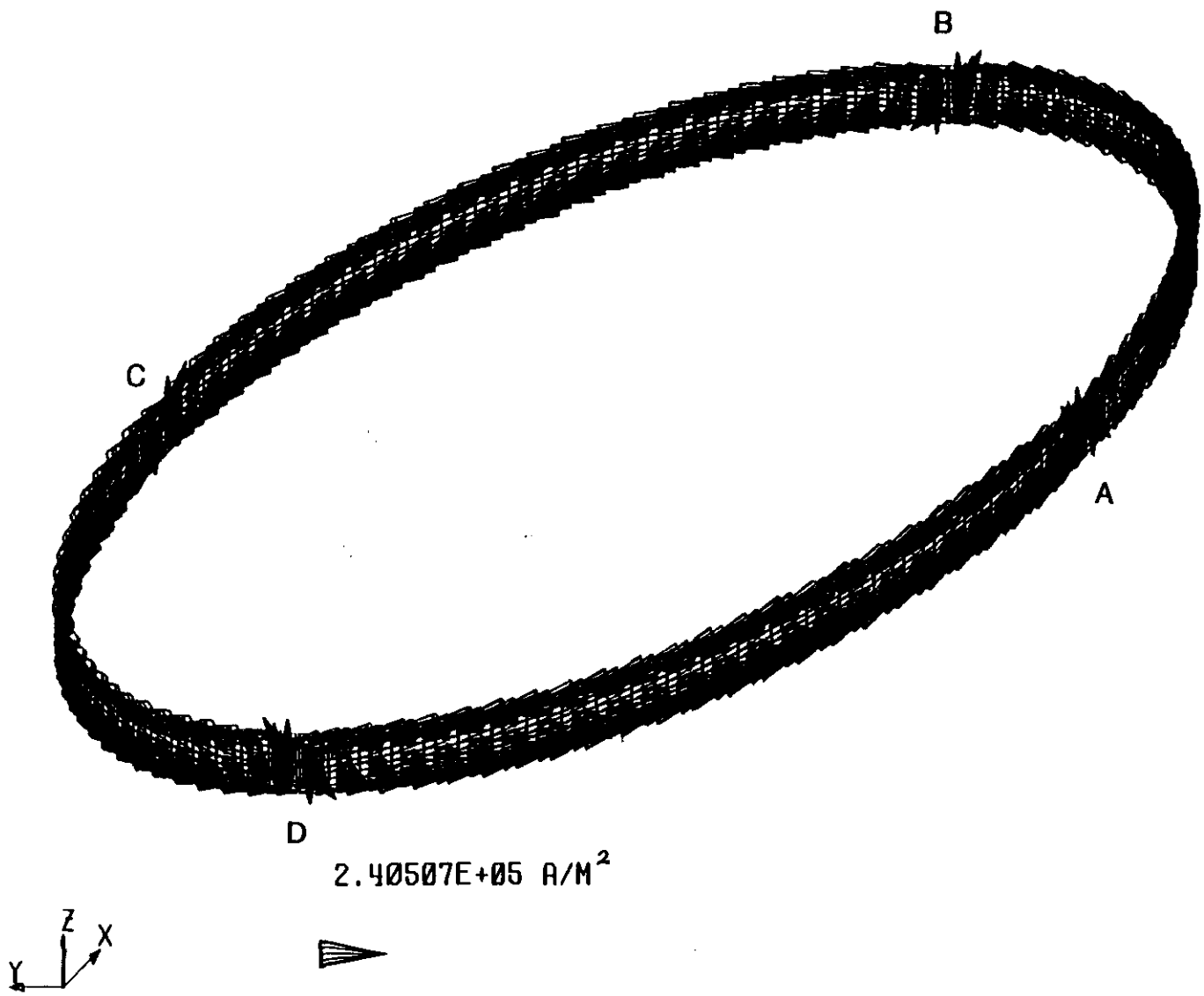

Fig. 6 Distribution of Current Density in the Tubing Jumpers of the 12-th Bobbin at t=9 s.

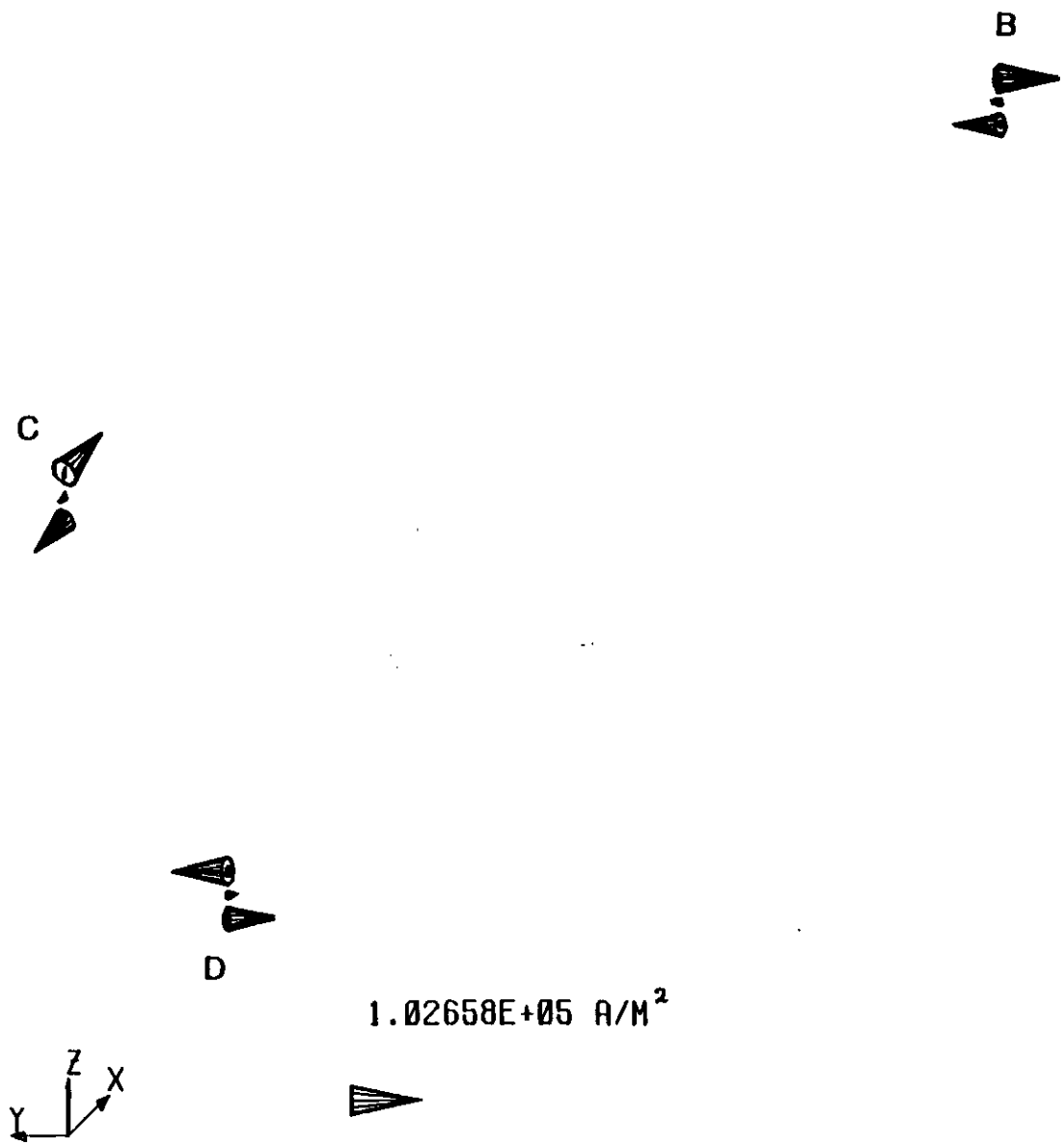

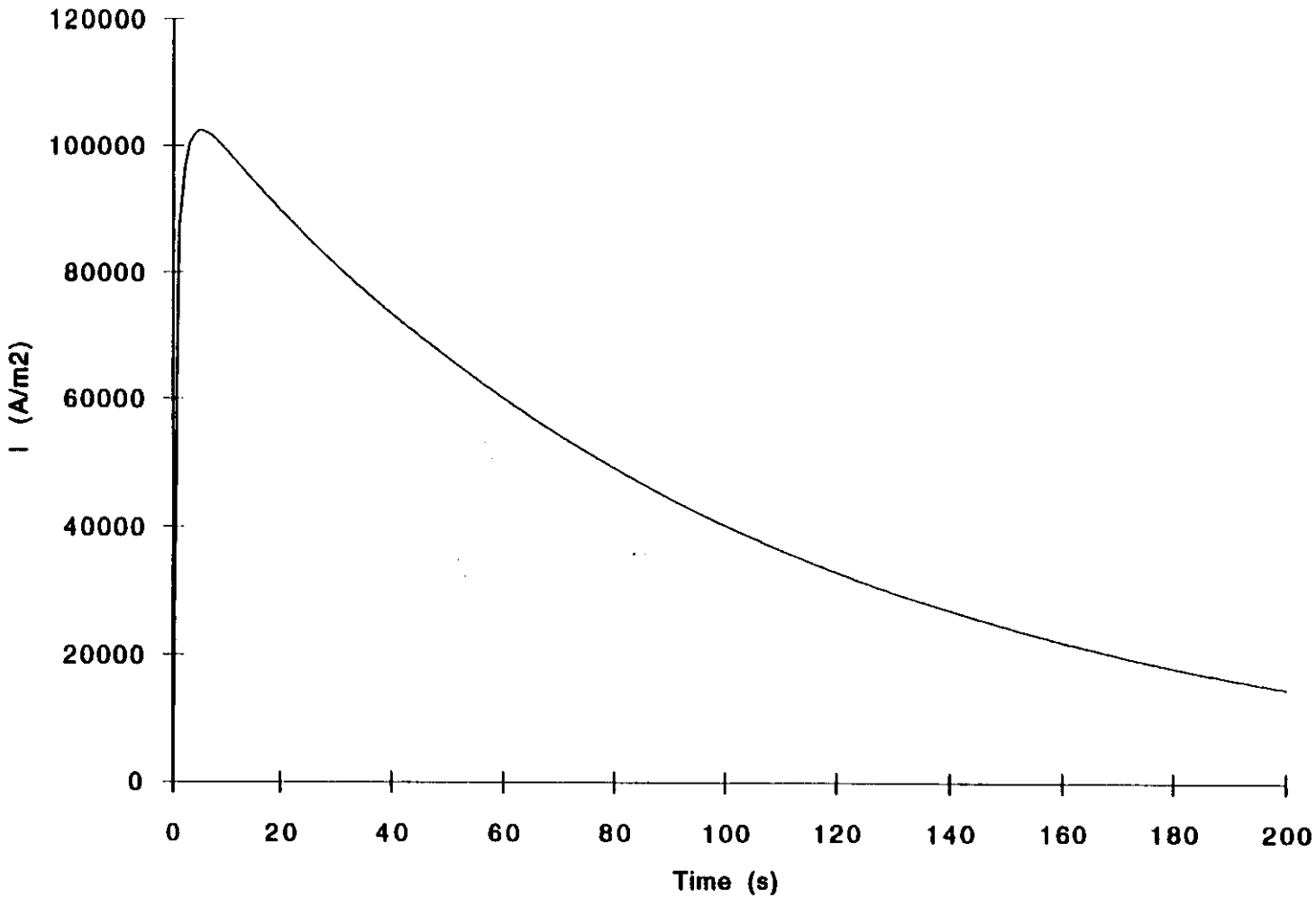

Fig. 7 Current Density in a Typical Outer Tubing Jumper

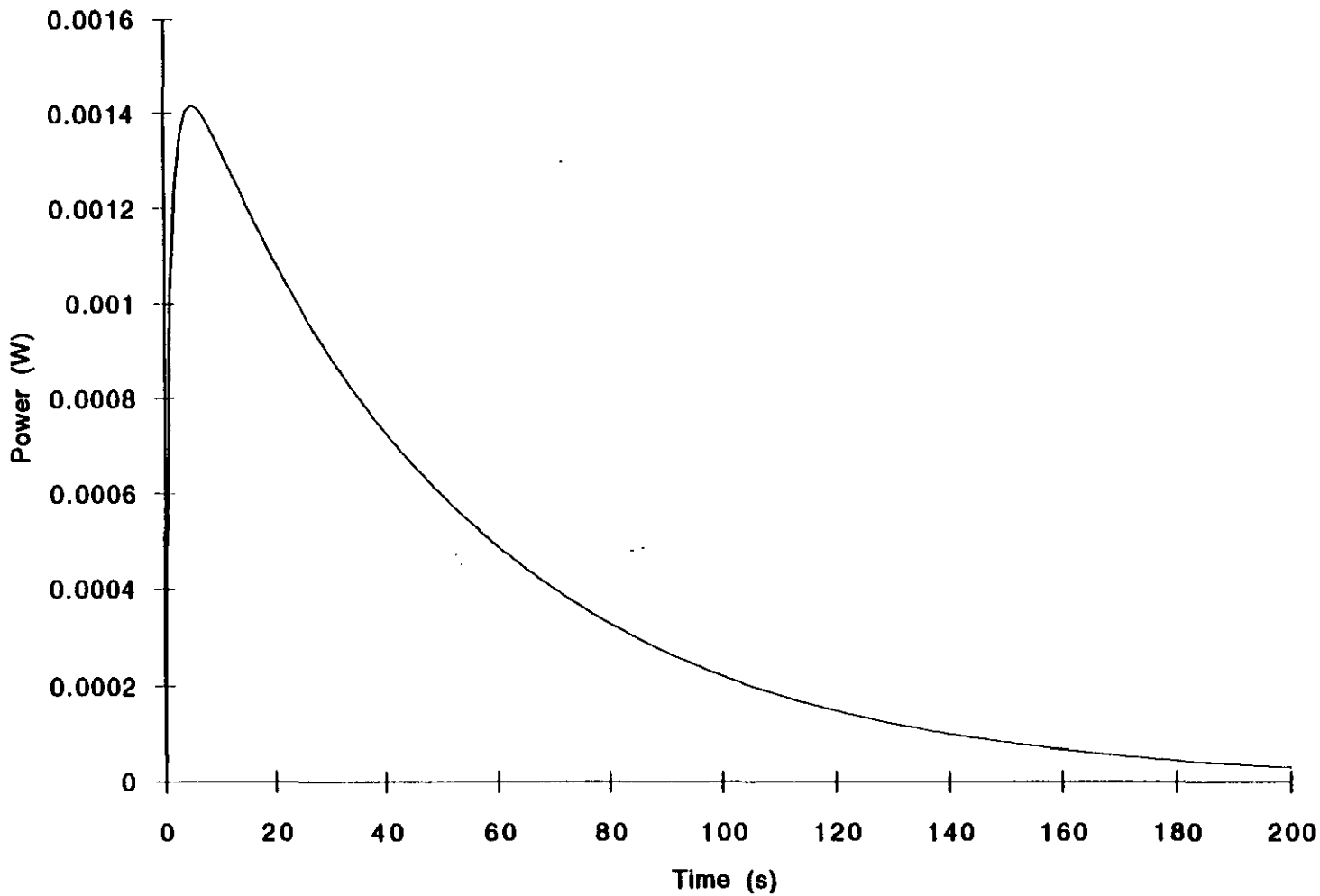

Fig. 8 Power Deposition in a Typical Outer Tubing Jumper